Less variability when growing faster? Experimental assessment of the relationship of growth rate with functional traits of the marine diatom *Phaeodactylum tricornutum*

Helena Cornelia Laurentia Klip ·
Cédric Léo Meunier · **Maarten Boersma**

Abstract Diversity and its drivers and consequences are at the heart of ecological research. Mostly, studies have focused on different species, but if the causes for increases or decreases in diversity are general, the observed patterns should also be observable within genotypes. As previous research shows that there is higher variability in nitrogen to phosphorus ratios (N/P) between slow-growing unicellular algal populations, compared to fast-growing ones, we expected to observe similar patterns within genetically identical strains growing at different rates. We tested this hypothesis in a laboratory experiment performed with a monoculture of the diatom *Phaeodactylum tricornutum*. Using a growth rate gradient obtained with 10 chemostats, we were able to determine the effect of growth rate on the diatom's elemental stoichiometry as well as on selected traits, such as cell size and shape. Our results showed indeed less intercellular variability (in the selected traits assessed on single-cell level) in the faster-growing populations, which was accompanied by a downward trend in bulk N/P ratios. We pose that this higher variability at lower growth rates potentially results in higher variability of the food sources available for higher trophic levels with potential consequences for the transfer efficiency of energy and matter in marine food webs.

Keywords Elemental stoichiometry · Intercellular · Phenotypic plasticity · Phytoplankton · Redfield ratio · Trait-based

H. C. L. Klip (✉) · C. L. Meunier · M. Boersma
Alfred-Wegener-Institut Helmholtz-Zentrum für Polar- und Meeresforschung, Biologische Anstalt Helgoland, Helgoland, Germany
e-mail: helena.klip@flbs.umt.edu

C. L. Meunier
e-mail: cedric.meunier@awi.de

M. Boersma
e-mail: maarten.boersma@awi.de

Present Address:
H. C. L. Klip
Flathead Lake Biological Station, University of Montana, Polson, MT, USA

M. Boersma
Naturwissenschaften 2, University of Bremen, Bremen, Germany

Introduction

Biodiversity and its drivers is one of the hot topics in current ecological research. Traditionally, much of the focus in studies on biodiversity was on different species, but recently intraspecific genetic diversity has attracted considerable attention (e.g. Reusch & Boyd, 2013; McGregor & Sendall, 2021).

One of the main reasons that (genetic) diversity has been so thoroughly studied, is the increasing loss of biodiversity (Cardinale et al., 2012) and its connection with ecosystem stability and food web efficiency (Thébault & Loreau, 2006). High biodiversity can act as a buffer against disturbances by stabilising the ecosystem (Thébault & Loreau, 2005), and it can increase the range of resource quality available for higher levels which benefits food web efficiency (Duffy et al., 2007; Moorthi et al., 2016; Plum & Hillebrand, 2019). Interestingly, phenotypic plasticity (i.e. intragenerational non-genetic trait variation within species) has been under much less scrutiny, whereby the processes that affect stability and trophodynamics should theoretically also hold when considering this kind of diversity. This aspect is particularly interesting to study in planktonic food webs, since phytoplankton exhibit a large degree of phenotypic variability. Phytoplankton take up nutrients, such as carbon (C), nitrogen (N) and phosphorus (P) separately, and as a result of their lack of homeostasis, they show a large diversity in nutrient contents which affects their quality as food for higher trophic levels.

Stoichiometric variation in nutrient content is not random, but related to the growth conditions of the algae. For example, Goldman et al. (1979) observed that at very high growth rates, variation in cellular N/P ratios among populations of phytoplankton decreased, and suggested that at these high growth rates, the Redfield ratio (Redfield, 1958), with a N/P of 16, acts as a global attractor. In other words, relative nutrient availabilities or quantities (dilution rates) can alter growth rates, which lead to different cellular N/P ratios (Rhee, 1978; Goldman et al., 1979). This would indicate that the Redfield ratio of C/N/P 106/16/1 is not only the average bulk value of seston, but that it represents an optimum cellular elemental ratio at high growth rates. A possible explanation for this phenomenon was given by Loladze & Elser (2011), who asserted that the N/P ratio of 16 represents the very core of cellular make-up with typical contributions of proteins (rich in N) and nucleic acids (rich in P). Only if the relative composition of those is optimal, can high growth rates be attained, or only at maximal growth rates does the composition of the organisms approach the Redfield ratio. In contrast, at lower growth rates this optimality cannot be expected, and as a result the variation in cellular N/P ratios at low growth rates is much higher (e.g. Rhee, 1978; Goldman et al., 1979; Geider & La Roche, 2002; Garcia et al., 2016): there are many ways to grow slowly, but only one way to grow fast. In other words, there are many ways in which cells can be limited in their growth, but there is only one optimal state in which they can reach their highest (maximum) growth rate, and as a result the diversity of biochemical make-up of primary producers is strongly related to their growth rates.

Not only does the variation in cellular N/P decline with growth rate, also the total value of the ratio approaches to Redfield (Redfield, 1958). As stated above, from a stoichiometric perspective, optimal growing conditions are those where neither N nor P are limiting, essentially representing the threshold between N limitation and P limitation (Droop, 1974; Rhee & Gotham, 1980; Thrane et al., 2016). Moreover, the growth rate hypothesis (GRH; Elser et al., 1996, 2008; Sterner & Elser, 2002) predicts a higher demand for P when growing fast as there is a higher need for P-rich ribosomal RNA to support elevated protein synthesis rates. Thus, high growth rate is related to higher amounts of P in the organism. In N-limited systems, however, N/P goes up with growth rate, albeit more constrained compared to P-limited systems (e.g. Klausmeier et al., 2004; Hillebrand et al., 2013; Garcia et al., 2016). Nevertheless, in the light of global change with predicted increasing N/P ratios (Peñuelas et al., 2012; Moore et al., 2018), the number and degree of natural systems with P limitation is expected to rise. This is due to enhanced thermal surface stratification causing lowered supply from deeper (nutrient-rich) water masses (Martiny et al., 2022), and by altered biogeochemical cycles with increasing imbalances in N/P ratios (Peñuelas et al., 2013). Consequently, there may be an increasing number of slower-growing algal cells with less optimal biochemical compositions.

Building on the original study of Goldman, the relationship between cellular N/P ratios and growth rate was further studied by Hillebrand and colleagues (2013), who conducted a meta-analysis on 43 datasets of different phytoplankton species from diverse functional groups in both mono- and polycultures. They corroborated Goldman's predictions and observed an overall convergence in the N/P ratio of bulk material approaching the Redfield ratio with increase in growth rate. They found, furthermore, that

there was less variability in cellular N/P ratios among fast-growing microalgal populations than among slow-growing ones.

If the explanation that slower growth rates a yield higher plasticity in cellular N/P ratios indeed holds, this should also be visible *within* populations or even *within* isogenic strains, i.e. in a fast-growing population, the variation in traits between genetically identical single-cells should be lower than the variation between cells in a slower-growing population. Hence, based on the results of Goldman et al. (1979) and Hillebrand et al. (2013), we hypothesise that, even within single strains, fast-growing cells should resemble each other more than they would at lower growth rates. This prediction has never been directly tested experimentally. So far, only the recent paper by Groß et al. (2021) hints in this direction, but in this study the growth rates were not controlled directly, but varied through changes in environmental conditions.

Answering the question above whether the patterns in intercellular trait variability and elemental composition with growth rate would also hold within a single genotype, is not merely a fascinating academic exercise, it also contributes to a deeper understanding of growth rate and its link to cellular traits (Litchman & Klausmeier, 2008; Isanta-Navarro et al., 2022). For instance, relatively slow-growing phytoplankton populations with large intercellular variability may offer a broad window of potential food items for herbivores to pick from (e.g. Meunier et al., 2012), but this has not yet been assessed on intercellular level in isogenic cultures.

Here, we experimentally assessed the influence of cellular growth rate of one single phytoplankton strain in the mean and variability of important planktonic traits, such as size, shape and the elemental composition of the cells. We assessed trait variability along a gradient of 10 different growth rates (0.1–1.0 d^{-1}) in a chemostat set-up. For this experiment, we selected the ubiquitous model diatom *Phaeodactylum tricornutum* Bohlin. This diatom is a polymorphic species with four morphotypes: fusiform, triradiate, oval and the rare cruciform, that is known to be able to reach relatively high growth rates (e.g. He et al., 2014; Xue et al., 2015). Since there is only one species in the genus *Phaeodactylum*, only the genus name will be used throughout the text. Our objective for this study was to investigate whether in

accordance with the studies by Goldman et al. (1979) and Hillebrand et al. (2013) faster-growing algal cells have lower cell-to-cell trait variability in elemental compositions and in other traits, such as cell size and pigment content.

Material and methods

In this study, we cultured the diatom *Phaeodactylum* in ten different chemostats with different growth rates and used a combination of bulk measurements to corroborate the general patterns of change with modified growth rates and individual measurements using flow cytometry and microscopy to assess the variation within cultures. The results from this study provide novel insights into the phenotypic plasticity within genotypes, besides the potential linkage between growth rate and other functional traits.

Experimental design

For this study, we grew the ubiquitous phytoplankton species *Phaeodactylum tricornutum* strain CCAP 1052/1A in chemostats. For the culturing of the diatom, medium was created using artificial seawater (Tropic Marine® Sea Salt CLASSIC; aerated overnight for mixing and to restore the carbonate system; salinity of 32), 0.2 μm sterile-filtered, and subsequently enriched to f/2 medium nutrient concentrations with a N/P molar ratio of 24.3 (Guillard & Ryther, 1962; Guillard, 1975) with the addition of 5 mg L^{-1} sodium fluorosilicate. The light intensity used was 100 μmol photons m^{-2} s^{-1} with continuous light (GHL Mitras Lightbar 2, Cold white, 6500 K). Stock cultures were pre-acclimated to these conditions for at least 10 generations. During the experiment, algal cells were grown in chemostats made of 1-L laboratory glass bottles placed on magnetic stirrer plates (setting 1, ~250 rpm, IKA) combined with gently sterile-filtered and humidified aeration (0.2 μm, Midisart® 2000, Sartorius Stedim Biotech, Göttingen, Germany & 0.2 μm 25 mm Acrodisc® CR Syringe Filter, PTFE Membrane, Pall Corporation) in a 20 °C temperature-controlled room.

We created a gradient consisting of 10 chemostats with different dilution (flow-through) rates, using peristaltic pumps (REGLO Digital, ISMATEC, Germany, 7×ISM831+3×ISM834)

ranging from 10 to 100% total volume displacement per day, based on the specific growth rate range of *Phaeodactylum*. More specifically, when the cultures reach steady-state, the dilution rate equals the growth rate. All pumps were calibrated in the days before the start of the experiment as recommended in the manufacturer's manual.

To initiate the differently growing populations, chemostats were inoculated with a 100-ml aliquot of the *Phaeodactylum* stock culture, and subsequently filled with medium to an end volume of 800 ml. The cultures were left for 72 h in the experimental setting to acclimate to the chemostats, i.e. aeration and gentle magnetic stirring, before starting the medium feed. First, all pumps were set in the middle of the dilution rate range. After another 48 h (5 d post-inoculation), the pumps were adjusted to the desired dilution rates (0.1–1.0 d^{-1}). Every other day, an aliquot (< 5 ml) was taken directly from the chemostats, and cell densities were determined using bench-top flow cytometry (BD Accuri C6, Becton Dickinson). When the cell densities of individual chemostats were constant for three consecutive measuring days, we established that steady state had been reached. Then, the samples were collected after at least another three generations (after observing steady-state conditions for the first time), leading to different individual harvest moments.

For the assessment of the potential linkage between growth rate and other functional traits, we sampled the algae to assess the following traits: elemental composition, pigment content, cell size, internal complexity of the cell shape (hereafter granularity) and morphotype. Due to the methodological challenges of measuring cellular elemental make-up of single-cells, we settled for a combination of single-cell measurements and bulk ones, because not all traits were amenable to individual measurements. Elemental contents were hence measured using bulk (retained on filters) samples, whereas pigment content, cell size, granularity and morphotype were assessed on individual cells, using flow cytometry and microscopy. More specifically, we used the relative values of the flow cytometric measurements (BD Accuri C6) using three detectors with the blue laser (488 nm), combined with morphotype counting from light micrographs.

Sample collection

At harvest, at least three generations after reaching steady state, we collected a sample of < 80 ml (10%) of the total volume (800 ml), to maintain the possibility to continue the chemostat cultures. We divided this aliquot as follows: (i) a 2-ml subsample for measuring with the flow cytometer for relative means and variation within cellular pigment content, cell size and cellular granularity; (ii) a minimum of 20 ml for filtering through a 0.2 μm (25 mm, Minisart® syringe filter, Sartorius Stedim Biotech GmbH, Göttingen, Germany) and storing at -20 °C until further analysis for dissolved nutrients determination; (iii) a varying subsample (based on the cell density) to assess total C, N and P on three filters; and (iv) the left-over for fixing with Lugol's iodine solution (1% v/v; Sigma-Aldrich; hereafter Lugol) for light microscopic analysis. For the elemental sampling, we utilised pre-combusted GF/F filters (5 h at 450 °C in the Heraeus muffle furnace) to retrieve the material. We dried one filter directly at 60 °C for later C and N analysis. The other two filters—for P and back-up—we stored in the -80 °C freezer, until further analysis. The fixed samples were stored in the dark at 4 °C, until further analysis.

Sample analyses

Cellular carbon and nitrogen quota were determined by combustion in a CHNS-analyser (Vario MICRO cube, Elementar), using acetanilide (C_8H_9NO) as the calibration standard. Phosphorus quota was measured by colorimetric analysis of orthophosphate (PO_4^{3-}) obtained by acidic oxidative hydrolysis, according to Grasshoff et al. (1999). Dissolved inorganic N sources of nitrate (NO_3^-) and nitrite (NO_2^-), and dissolved PO_4^{3-} were analysed using a SEAL Autoanalyzer 3 High Resolution, according to the methods of Grasshoff et al. (1999). We decided to not measure the macronutrient silicate in this study, because this is only utilised by *Phaeodactylum*, when they are in their oval cell shape (e.g. Borowitzka & Volcani, 1978; Brzezinski et al., 1990).

The intercellular trait variation within cultures of pigment content, cell size and granularity was assessed using the Accuri software CFlow Plus version 1.0.264.15. The flow cytometer is equipped with two lasers, a common air-cooled blue

argon-ion laser (488 nm excitation) and a red diode laser (640 nm excitation), from which we used the first one. After excitation at this wavelength, the autofluorescence of the cellular pigment content emits at a wavelength of > 670 nm (red fluorescence; emission detector FL3; e.g. Marie et al., 2005). This excitation wavelength can detect the pigments chlorophyll *a* and *b*, carotenoids, xanthophyll and peridinin (Rogers et al., 2012), from which chlorophyll *a* and *β*-carotene are known to be synthesised by *Phaeodactylum* (e.g. Carreto & Catoggio, 1976). To simplify this, we used this autofluorescence signal (obtained by FL3) as a composite estimate of pigment content, most of which is chlorophyll *a*. The scatter detectors were used with forward scatter (FSC; $0° \pm 13$) as a proxy for cell size, and side scatter (SSC; $90° \pm 13$) as a proxy for cellular granularity. We assessed the cellular granularity, which is a measure for the internal complexity of the cells, i.e. basically of the concentration of material in their cytoplasm.

In the cytograms produced by flow cytometry, the clusters corresponding to the fresh *Phaeodactylum* populations were automatically enumerated by drawing regions around them, which were clearly distinguishable event clusters from the background noise. The number of events within them was noted. We could, however, not distinguish different morphotypes within such regions. Subsequently, the means and the corresponding relative coefficients of variation (CVs in %; $CV = SD/mean*100$) of the clusters (one per chemostat culture) were noted with plotting FSC against FL3, and for the granularity SSC versus FL3. They were noted both in arbitrary units (a.u.) and in percentages. We used the means and variability reported from the flow cytometer. Our cell size and cellular granularity determinations were based on the mean FSC and SSC counts per algal population of at least 1,000 assessed cells, respectively.

The diatom *Phaeodactylum* is a known polymorph, hence an ideal candidate to study intercellular variability and phenotypic plasticity. We assessed the cell morphometry in the subsamples that were fixed with Lugol using a camera (AxioCam HRc, Zeiss) coupled to an inverted microscope (Observer A1, Zeiss) combined with software (Axiovision SE64, Rel. 4.9, Zeiss). The subsamples were transferred into Utermöhl chambers and left for at least 8 h to settle (Utermöhl, 1958). We determined *Phaeodactylum* cell shapes on at least five light micrographs showing a minimum of 1,000 cells in total for the following cell shapes: fusiform, triradiate, oval and cruciform, following He et al. (2014).

Statistical analyses

We collected and processed the data for assessment of the intercellular variability of the cells and their potential growth limitations as follows: (i) all the presented CV values were directly obtained from the CFlow Plus software (BD Accuri™, version 1.0.264.15); and (ii) the variability in the morphometric distribution we described by the Shannon–Wiener diversity index (H'; Weaver & Shannon, 1963).

Data visualisations and statistical analyses were performed in the software SigmaPlot version 12.3 (Systat Software Inc., San Jose, CA, USA). All analyses were carried out using an exponential regression type analysis, using the complete gradient of growth rates. A 3-parameter exponential regression was fitted through all the data to allow for a nonlinear response to growth rate, as well as the fact that none of the variables measured can become negative, which cannot be avoided with simple linear regressions. Statistical significance was considered when $P < 0.05$.

Results

Growth conditions

During harvest, subsamples were collected for dissolved nutrient analyses of NO_3^-, NO_2^- and PO_4^{3-}. The measured dissolved nutrient concentrations can be found in S1 Table. The cell densities at this moment varied from 600,000 to 1,400,000 cells ml^{-1} with no clear trend in density varitation, indicating that the maintained cellular growth rates were a result of different dilution rates in the chemostats—as an environmental cue (S1 Fig.).

Functional traits

To determine the cellular elemental stoichiometry within the different chemostats, we measured

particulate macronutrients C, N and P (S2 Table). We observed a downward trend along the growth rate gradient for all three ratios: N/P ($R^2 = 0.70$, $P = 0.0086$), C/N ($R^2 = 0.96$, $P < 0.0001$) and C/P ($R^2 = 0.94$, $P < 0.0001$; Fig. 1). These trends suggest that there is an optimal ratio at any growth rate, but that the optimum declines towards Redfield values at high growth rates. With higher growth rates, elemental cellular compositions approached the Redfield ratio.

The assessment of the mean and the relative variability of pigment content, cell size and cellular granularity within one single strain indicated in general that fast-growing populations have indeed lower cell-to-cell variation (Figs. 2, 3). To aid explaining the intercellular variation assessment via flow cytometry, we included three examples of zoomed-in cytograms and their corresponding event spreads (Fig. 2). For the autofluorescent signal representing an estimation of the relative cellular pigment content, there is no significant response in the mean pigment content along the gradient ($R^2 = 0.36$, $P = 0.17$, Fig. 3A), and a significant downward trend in the coefficient of variation from 143.4% for the slowest-growing population to 40.6% for the fastest one ($R^2 = 0.86$, $P = 0.0001$, Fig. 3B). For the relative cell size, there is no significant response in the mean size along the gradient ($R^2 = 0.018$, $P = 0.92$, Fig. 3C), and again a significant downward trend in the cell-to-cell variation from 124.2% for the slowest-growing population to 75.6% for the fastest one ($R^2 = 0.92$, $P < 0.0001$, Fig. 3D). For cellular granularity, we found a statistically significant downward trend in the mean cellular granularity ranging from 378,555 to 54,684 a.u. ($R^2 = 0.98$, $P < 0.0001$, Fig. 3E), and also negative trend in cell-to-cell variation along the growth rate gradient, albeit in this case a non-significant one ($R^2 = 0.28$, $Pp = 0.23$, Fig. 3F).

Cell morphometry

Light microscopic assessment of the fixed samples showed a minor shift in relative distribution in morphotypes and an increase in cell morphological diversity in faster-growing populations based on regression type analyses (Fig. 4). For the slowest-growing population, the relative abundance of cells in fusiform shapes was 96.2% compared to 90.0% for the fastest-growing population. For the oval and triradiate shapes, there were increases of 1.6 and 4.6% between
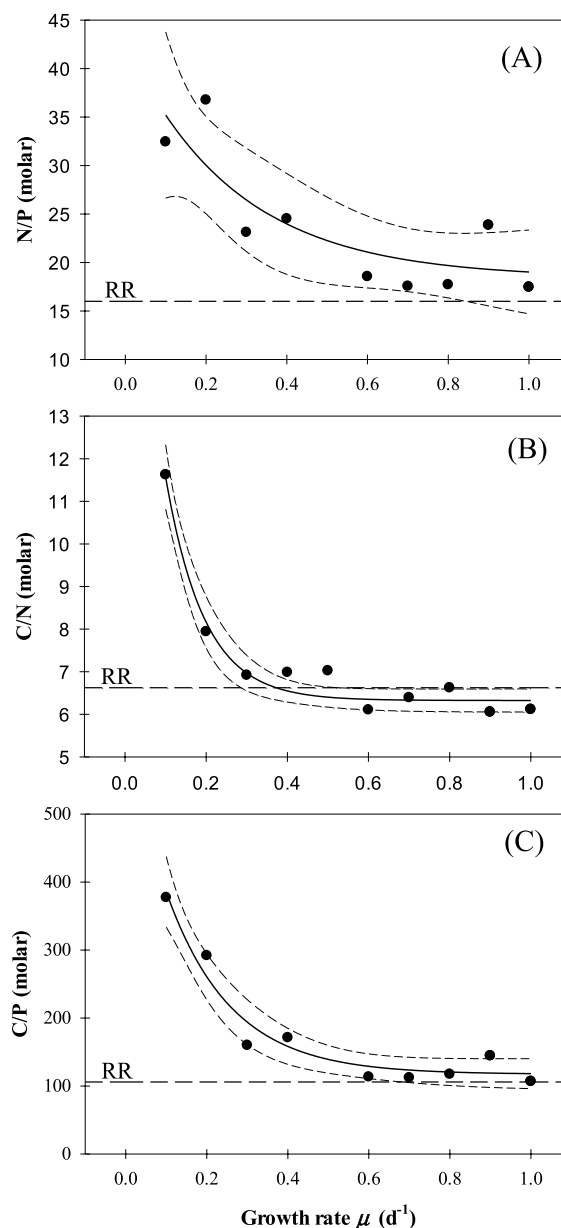

Fig. 1 Cellular particulate macronutrient ratios depicted with black solid circles (**A**–**C**) of the N/P (**A**), C/N (**B**) and C/P (**C**) ratios along the growth rate gradient. We fitted exponential decay regression models for all three ratios. The P content of the 0.5 d^{-1} population was too low with 0.15 pg $cell^{-1}$, which led to unrealistically high N/P and C/P ratios. Hence, the corresponding values got discarded from all further analyses. We added short-dashed lines depicting the 95% confidence intervals. The black horizontal long-dashed lines represent the Redfield ratio (RR)
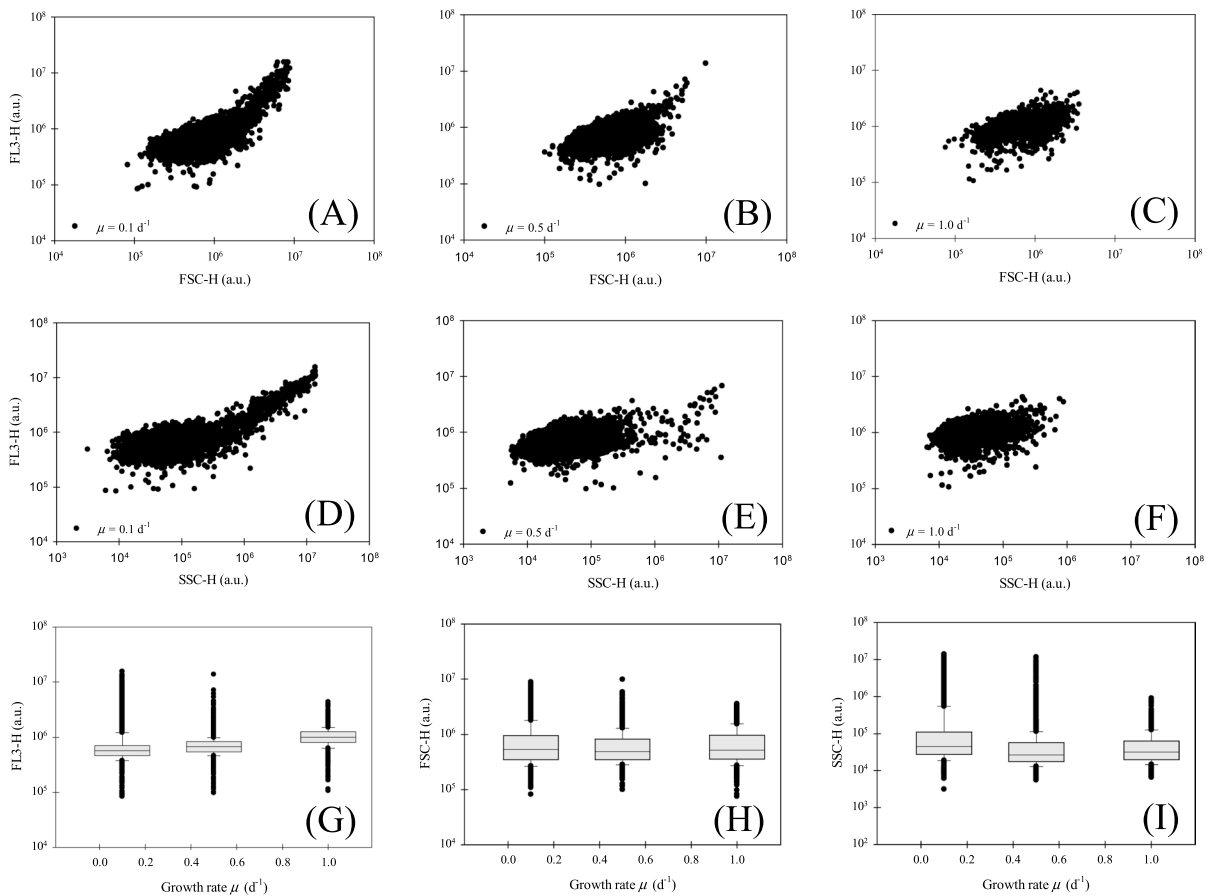
Fig. 2 Three visualisation examples of slow-, intermediate- and fast-growing populations using zoomed-in cytograms on *Phaeodactylum* of log-transformed forward scatter (FSC-H; proxy for cell size) over FL3 channel (FL3-H; proxy for grouped pigment content; **A–C**), of side scatter (SSC-H; proxy for cellular granularity) over FL3 channel (**D–F**) and the corresponding event spreads including boxplot presentation (**G–I**). Each dot represents a registration event by the flow cytometer of a single *Phaeodactylum* cell

the slowest and fastest-growing populations, respectively. There was variation in the minor shift in relative morphotype distribution along the growth rate gradient. Regarding the cell shape diversity, based on the regression model, the Shannon–Wiener diversity index went up with growth rate, as slower-growing *Phaeodactylum* populations ($\mu = 0.1$–0.5 d^{-1}) mainly consist of cells in their fusiform, while in the faster-growing populations ($\mu = 0.6$–1.0 d^{-1}) more cells shift to their triradiate and oval shapes, which led to a higher diversity index value of 0.19 along the gradient (Fig. 4). Overall, we observed an upward trend in cell shape diversity ($R^2 = 0.63$, $P = 0.012$) along the growth rate gradient. However, we acknowledge that there is variation around this regression line, and

thereby within the upward trend. During the assessment of the light micrographs, we observed no cells in their rare cruciform shape.

Discussion

Here, we assessed whether faster-growing cells of one genotype of the marine diatom *Phaeodactylum* had elemental ratios approaching the Redfield ratio, as predicted by Goldman et al. (1979), as well as lower intercellular trait variability as predicted by Hillebrand et al. (2013). We showed that our hypotheses of downward trends (in P-limited systems) with increase in growth rate in N/P indeed
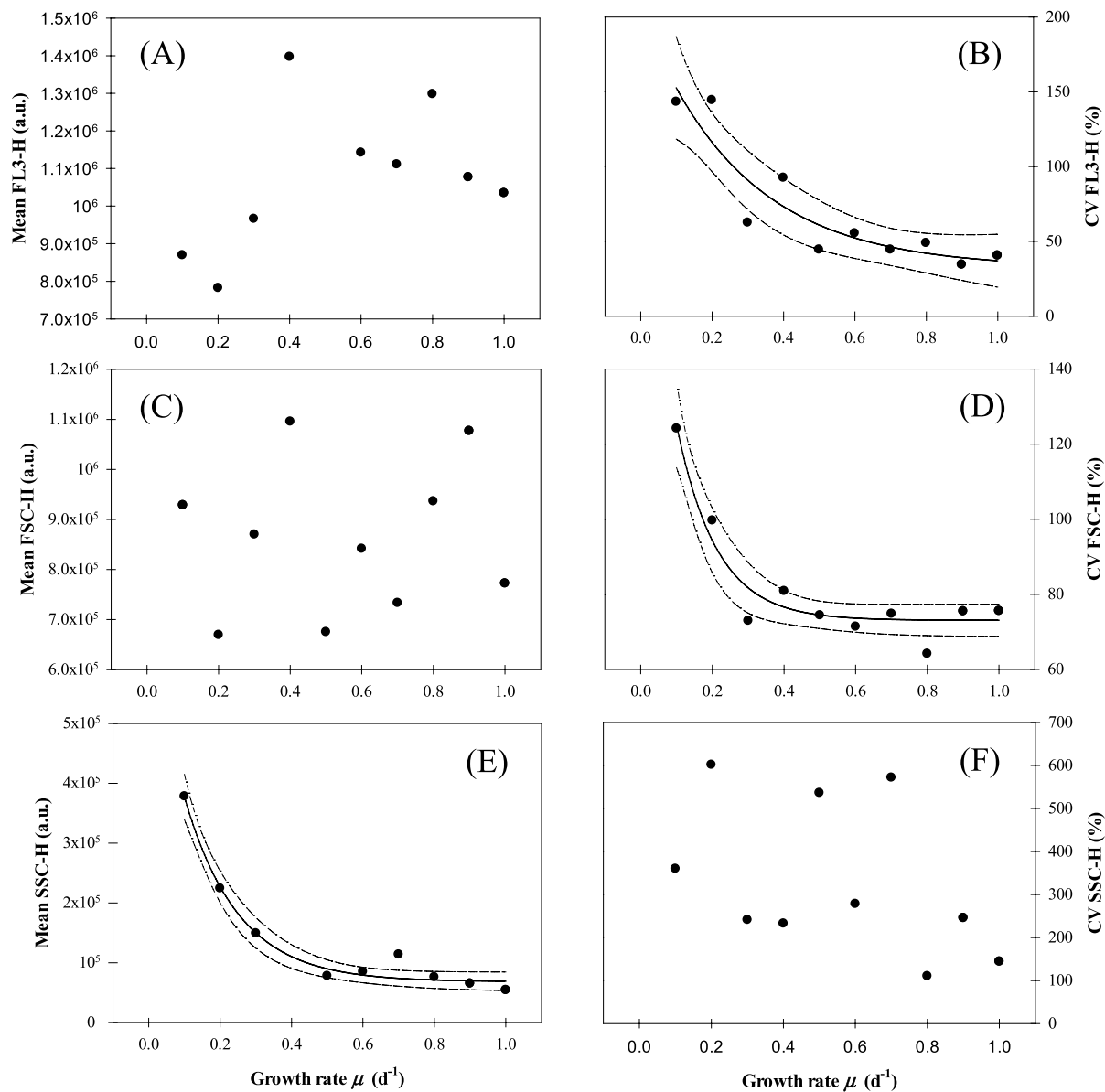
Fig. 3 Assessment of the mean (in arbitrary units; a.u.) and the relative CV (in %) of the pigment content (A + B), cell size (C + D) and cellular granularity (E + F) along the growth rate gradient using exponential regression models. Each circle represents one chemostat population. Where for mean pigment content an exponential rise to maximum model and for all other plots exponential decay regressions were significant, we indicated this by adding the corresponding regression lines through these measurements combined with 95% confidence intervals showed with the black short-dashed lines. Noteworthy, despite the fact that all measurements displayed in this figure were detected concurrently by the flow cytometer, we discarded for the mean pigment content and the mean cellular granularity (A + E) all substantially deviating measured values of 720,748 a.u. at 0.5 d^{-1} and 550,059 a.u. at 0.4 d^{-1}, respectively, from all further analyses

approached the Redfield ratio, as well as most of the cell-to-cell variability, were met, and also hold true within populations of a single algal genotype.

We aimed to link several functional traits—elemental stoichiometry, cell size and shape and cellular pigment content and complexity—to growth rate. For the bulk elemental stoichiometric ratios (C/N/P), we

Fig. 4 Relative distribution of three present cell shapes in the differently growing *Phaeodactylum* populations and their corresponding Shannon–Wiener diversity index (H') values plotted in blue. We included three drawings of the corresponding shapes retrieved from www.biorender.com in the legend. We fitted through the H' values an exponential growth regression model combined with 95% short-dashed confidence intervals along the growth rate gradient
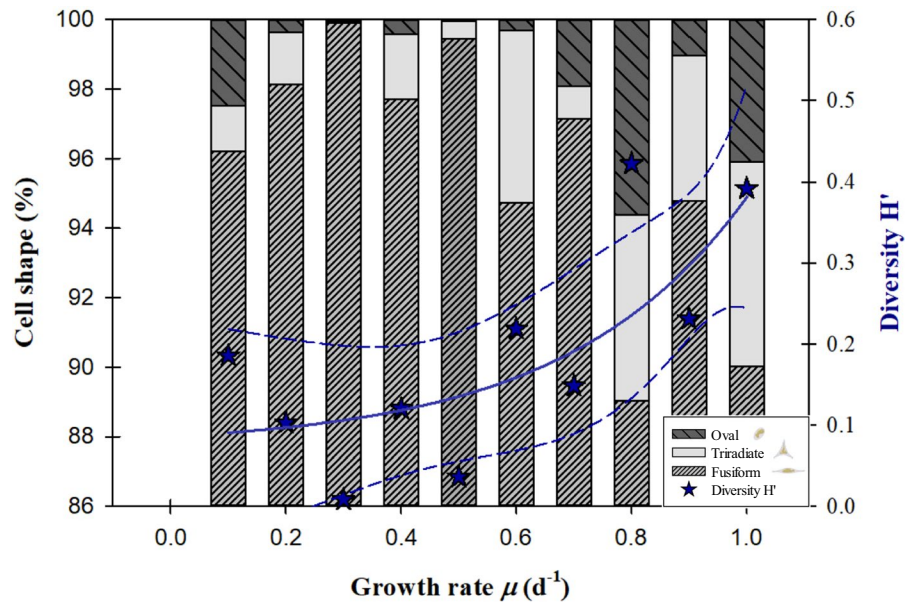
observed downward trends in all ratios with elevated μ. We found that the faster-growing algal populations contained more phosphorus (P), as predicted by the growth rate hypothesis for P-limited systems (Sterner & Elser, 2002; Flynn et al., 2010). These results agree with previous chemostat experiments, assessing three algal species from distinct marine taxa, a marine cyanobacterium *Synechococcus* sp. and one freshwater green alga *Selenastrum minutum* (Nägeli) Collins (Goldman et al., 1979; Elrifi & Turpin, 1985; Garcia et al., 2016). In the study by Maat et al. (2014), this drop in stoichiometric ratios was also observed in the fast-growing chemostat populations ($\mu = 0.70$ d^{-1}) compared to the slow-growing chemostat ones ($\mu = 0.23$ d^{-1}) for the marine picoplankter *Micromonas pusilla* (Butcher) Manton & Parke.

The measured stoichiometric elemental ratios of the model diatom *Phaeodactylum* were all approaching the Redfield ratio at high growth rates. This is in agreement with the work by Goldman et al. (1979), Loladze & Elser (2011) and Hillebrand et al. (2013), which overall hypothesised that when species grow faster, the ratios of their particulate elemental composition are converging to the Redfield ratio as global attractor, as a N/P of ~16 is intrinsically rooted in growth physiology (Loladze & Elser, 2011). This specific ratio is linked to the average N and P pools of all major macromolecular compounds of a phytoplanktonic cell growing at its maximum

rate under optimal growth conditions, when there is a balance of these compounds (Loladze & Elser, 2011). Moreover, a comparable cellular convergence in N/P ratio to Redfield with higher growth rate was also observed in, e.g. Rhee (1978) and Garcia et al. (2016). We linked for the first-time intercellular trait variation to elemental stoichiometric compositions.

Our results show lower intercellular variability in traits when the model diatom *Phaeodactylum* grew faster. To determine the within-culture intercellular variability, we estimated three functional traits, pigment content, cell size and cellular granularity using flow cytometry and one, cell shape, using microscopy. For the traits analysed by flow cytometry, we indeed observed decreasing variability with growth rate for pigment content and cell size. Thus, as was the case for the observations between cultures, variation also decreases within cultures. In contrast, and somewhat unexpectedly, the pattern with cell shape was opposite, with higher diversity at higher growth rates.

An increasing number of studies have investigated intraspecific variability between and within genotypes of one species (e.g. Kremp et al., 2012; Garcia et al., 2016; Brandenburg et al., 2018; Groß et al., 2021). Most studies observed both intraspecific variability and intrastrainal variability, but concentrated on solely bulk measurements on isogenic population level. The big difference with our study is that

we combined similar bulk measurements with measurements on intercellular level to corroborate potential trends between intercellular variability and growth rate.

There are several potential explanations for enhanced intercellular trait variability at lower growth rates. The first three potential explanations might be more study flaws, while the last two form more realistic ecological explanations. *First*, potentially, as a result of the very fast growth, cells are typically dividing synchronously, which would make them more similar to each other than cells that have lower division rates and co-occur in different stages of the division process (Massie et al., 2010). *Second*, the intercellular variability could have been caused by the culture regime, as chemostats also simultaneously control the mortality rate/residence time and hence determine the duration individual cells spend in the culture vessels. High dilution rates (high growth rates) create a population of young individuals, most likely with similar traits. Lower dilution rates will also allow older individuals to remain in the vessels. If trait variation is related to age variation, then we would expect the variation to indeed decrease with increase in growth (dilution) rates. However, the recent study by Groß et al. (2021) reported lowered intercellular trait variability with higher growth rate induced by global change related treatments of a single genotype diatom kept in batch, when residence time does not play a role. *Third*, the results might be snap shots of phenotypic selection towards optimal phenotypes in the slower-growing populations as well, i.e. the slower-growing populations might have been in a transitional state towards specific optimality at the time of the harvest eventually obtained via competitive exclusion. Despite the fact that we used a monoculture with one genotype, the phenotypic trait values are obviously not all exactly the same, e.g. there is always some spread in cell size among cells, due to distinct phases of cell division and slight variation in environmental cues. In other words, there was likely some phenotypic variation present in the chemostat inoculum that got sorted via intraspecific competition among diverse phenotypes. The latter could be tested by running the same experiment longer. *Fourth*, part of the increased intercellular variability is a result of enhanced stickiness of the cells caused by amplified C-excretion (at lower growth rates) to buffer non-optimal internal elemental

compositions (e.g. Engel, 2000; Klein et al., 2011). Cells sticking to each other would increase both overall cell size and cellular pigment content as well as cellular granularity, which we observed in the cytograms (i.e. the tails in the upper right corner), and which could be linked to slightly elevated organic material fluxes in the oceans (e.g. Fowler & Knauer, 1986). *Fifth,* under more favourable growth conditions (higher growth rate) there is a low demand for plasticity, for example, in nutrient acquisition strategies, leading to lower intercellular variability in those traits (e.g. West-Eberhard, 2003; Collins & Schaum, 2021). *Last*, at high growth rates everything is optimal (Loladze & Elser, 2011), as otherwise the cells could not be growing so fast, and as a result all the cells should be similar in their biochemical make-up. Irrespective of the explanation, the pattern is clear, and could have repercussions on ecosystem functioning (see below).

The higher diversity in shape at higher growth rates is less pronounced than the other traits assessed in this study and difficult to explain. Essentially the fusiform shape is being replaced by the two other forms in more or less equal amounts at higher growth rates, which increases the shape diversity via *morphotype sorting*. One of the biggest consequences of shape change is the change in surface area-to-volume ratio (SA/V). Cells in their triradiate shape have a higher SA/V (Bartual et al., 2008) and hence an increase in nutrient uptake efficiency (Thingstad et al., 2005; Litchman et al., 2007) and oval-shaped cells a lower SA/V with a reduced uptake efficiency. Noteworthy, larger cells with more vacuoles can store more macromolecular compounds (e.g. Thingstad et al., 2005). Thus, when *Phaeodactylum* is growing slower, fusiform cells with an intermediate SA/V increase in relative abundance, potentially in a trade-off of balancing nutrient uptake and storage, as these cells also had the highest granularity, indicating that they were storing large amounts of especially carbon in the cells. Song et al. (2020) determined that fusiform-shaped cells are rich in C-rich lipids and carbohydrates (i.e. cellular building blocks partly determining cell size), while oval-shaped cells were rich in N-rich proteins and pigments (i.e. linked to the autofluorescent pigment signal). Thus, the differences in shapes might be the consequences of the need for storing different compounds (carbon in the nutrient-limited slow growers and nitrogen and phosphorus

in the fast growers). We showed that the populations which were dominated by fusiform-shaped cells were also C-richer. Moreover, these populations had higher cellular granularity values. All in all, it seems that in our study the dominant growth strategy under less optimal growth conditions was luxury consumption combined with storage, which as a consequence of these demands led to fusiform-shaped cells. This strategy led to fuller cell compartments with macromolecular (carbon) compounds and hence elevated mean cellular granularity levels under less favourable growth conditions that led to reduced growth rates. At higher growth rates, the storage demands were lower and different, and hence the pressure of fusiform shape relaxed.

In the ecological literature, the diversity of prey availability has been linked to the stability of ecosystems, efficiency of food chains and much more. Especially phytoplankton diversity has received a lot of attention (Hillebrand & Matthiessen, 2009; Striebel et al., 2016), with strong foci on species diversity. Here, we show that even within genetically identical strains of one phytoplankton species diversity (i.e. trait plasticity) is possible, and this diversity is predictably dependent on the growth rate of the cells. Thus, depending on the growth rate of primary producers, the present prey offers different quality to their grazers. This might have consequences. For instance, the study by Malzahn & Boersma (2012) tested the influence of these C/N/P ratios on copepod's ontogeny. When they fed the calanoid copepod *Acartia tonsa* Dana, 1849 with P-rich and P-poor prey items of the same unicellular algal strain, they observed that its growth was delayed, when the copepod was feeding on high C/P food. Thus, a faster-growing algal population could lead to elevated growth rates of higher trophic levels as they present a higher quality food (e.g. Malzahn et al., 2007). So far, one grazing study hints in this direction showing how altered growth rates of two phytoplankton species impact the C transfer efficiency in the marine heterotrophic dinoflagellate *Oxyrrhis marina* Dujardin with the highest C transfer efficiency when fed with the fast-growing algal prey species (McBeain & Halsey, 2018). This link between algal prey growth rate and C transfer efficiency in zooplankton demonstrates that nutrient limitation can ultimately impact the amount of primary production lost in the ecosystem (Hantzsche & Boersma, 2010;

McBeain & Halsey, 2018). At the same time, since it is known that most zooplankton can feed selectively, i.e. they can actively select for specific prey with the food quality that meets their nutritional demands (e.g. Meunier et al., 2012), the higher variation (phenotypic diversity) at lower growth rates might create windows of opportunity for a more diverse set of grazers, thus potentially lower growth in the primary producers would be able to sustain a more diverse grazer community. Another potential ecological implication of differently growing algae is their effect on production of their corresponding viruses (Bratbak et al., 1993; Clasen & Elser, 2007; Maat et al., 2014). Viral production is sensitive to both phosphorus and nitrogen limitation, as P- or N-depleted viral hosts lead to lowered production in viruses (Maat & Brussaard, 2016). Thus, viruses would proliferate better, when infecting fast-growing host cells, and the rate at which specific algal populations are growing can also control the speed and impact of the top-down regulation by viruses in the field (Bratbak et al., 1993; Brussaard et al., 1995). In other words, infecting slow-growing algal cells that are C-richer would lead to higher DOC releases per lysed algal cell altering the structure of the microbial loop on ecosystem level (Azam et al., 1983; Lønborg et al., 2013).

On a broader scale, functional diversity in plankton communities is positively correlated with community stability, productivity, resource use efficiency and resistance to environmental pulse disturbances, such as storm and heatwave events, albeit negatively to resilience (Ptacnik et al., 2008; Baert et al., 2016; Vallina et al., 2017). The results could have important repercussions for our understanding of the availability of diverse foods as well as of selective feeding by grazers and of the corresponding population dynamics, such as the outcomes of competition during planktonic bloom events with overall elevated growth rates (Rhee & Gotham, 1980), especially as phytoplanktonic traits have different ecological functions, e.g. cell shape for resource acquisition and predator avoidance (Litchman & Klausmeier, 2008).

The work presented here might have benefitted from the following aspects. *First*, precision in the results could have been increased by adding biological replicates in the gradient design. *Second,* since we used an exponentially growing and well-acclimated (to frequently used experimental conditions) stock

culture for the experiment, we argued that the initial morphotype composition was mainly composed of regularly observed fusiform-shaped *Phaeodactylum* cells (Volcani, 1981; Martino et al., 2007). We could have checked the intrapopulation morphotype composition of the inoculum. *Last,* we could have run the experiment for a longer duration, since there are multiple definitions of steady-state conditions and for reason discussed above (third potential explanation). It is, furthermore, important to note that in the field, phytoplankton can behave differently due to other environmental cues, since the planktonic food web is more complicated than single species chemostat studies. Nevertheless, simplified and highly controlled laboratory experiments form good starting points for hypothesis testing. Future studies can add more complexity (i.e. trophodynamics and community structure) to the system or focus on the aforementioned follow-up question on the implications at different rates growing algal prey for higher trophic levels.

In summary, in non-genetic within species diversity (phenotypic plasticity), related to the growing conditions of the phytoplankton, constrained trait variation combined with convergence towards a singular value in the direction of the Redfield ratio is real. It has the potential to affect higher trophic levels, both by changing the overall availability of nutrients in the food as well as affecting the variation of potentially available prey. These findings contribute to our understanding of planktonic trophodynamics, and provide fine-tuning implications for ecological food web models.

Data availability The datasets generated during the study are going to be made available in the PANGAEA repository.

Declarations

Conflict of interest The authors have no competing interests to declare that are relevant to the content of this article.

References

Azam, F., T. Fenchel, J. G. Field, J. Gray, L. Meyer-Reil & F. Thingstad, 1983. The ecological role of water-column microbes in the sea. Marine Ecology Progress Series 10: 257–263. https://doi.org/10.7208/chicago/9780226125534-024.

Baert, J. M., F. De Laender, K. Sabbe & C. R. Janssen, 2016. Biodiversity increases functional and compositional resistance, but decreases resilience in phytoplankton communities. Ecology 97: 3433–3440. https://doi.org/10.1002/ecy.1601.

Bartual, A., J. A. Galvez & F. Ojeda, 2008. Phenotypic response of the diatom *Phaeodactylum tricornutum* Bohlin to experimental changes in the inorganic carbon system. Botanica Marina 51: 350–359. https://doi.org/10.1515/BOT.2008.047.

Borowitzka, M. A. & B. E. Volcani, 1978. The polymorphic diatom *Phaeodactylum tricornutum*: Ultrastructure of its morphotypes. Journal of Phycology 14: 10–21. https://doi.org/10.1111/j.1529-8817.1978.tb00625.x.

Brandenburg, K. M., S. Wohlrab, U. John, A. Kremp, J. Jerney, B. Krock & D. B. Van de Waal, 2018. Intraspecific trait variation and trade-offs within and across populations of a toxic dinoflagellate. Ecology Letters 21: 1561–1571. https://doi.org/10.1111/ele.13138.

Bratbak, G., J. K. Egge & M. Heldal, 1993. Viral mortality of the marine alga Emiliania huxleyi (Haptophyceae) and termination of algal blooms. Marine Ecology Progress Series 93: 39–48.

Brussaard, C., R. Riegman, A. Noordeloos, G. Cadée, H. Witte, A. Kop, G. Nieuwland, F. Van Duyl & R. Bak, 1995. Effects of grazing, sedimentation and phytoplankton cell lysis on the structure of a coastal pelagic food web. Marine Ecology Progress Series 123: 259–271. https://doi.org/10.3354/meps123259.

Brzezinski, M. A., R. J. Olson & S. W. Chisholm, 1990. Silicon availability and cell-cycle progression in marine diatoms. Marine Ecology Progress Series 67: 83–96.

Cardinale, B. J., J. E. Duffy, A. Gonzalez, D. U. Hooper, C. Perrings, P. Venail, A. Narwani, G. M. Mace, D. Tilman & D. A. Wardle, 2012. Biodiversity loss and its impact on humanity. Nature 486: 59–67. https://doi.org/10.1038/nature11148.

Carreto, J. & J. Catoggio, 1976. Variations in pigment contents of the diatom *Phaeodactylum tricornutum* during growth. Marine Biology 36: 105–112. https://doi.org/10.1007/BF00388433/.

Clasen, J. L. & J. J. Elser, 2007. The effect of host Chlorella NC64A carbon: phosphorus ratio on the production of Paramecium bursaria Chlorella Virus-1. Freshwater Biology 52: 112–122. https://doi.org/10.1111/j.1365-2427.2006.01677.x.

Collins, S. & C. E. Schaum, 2021. Growth strategies of a model picoplankter depend on social milieu and p CO2. Proceedings of the Royal Society B 288: 20211154. https://doi.org/10.1098/rspb.2021.1154.

Droop, M., 1974. The nutrient status of algal cells in continuous culture. Journal of the Marine Biological Association of the United Kingdom 54: 825–855. https://doi.org/10.1017/S002531540005760X.

Duffy, J. E., B. J. Cardinale, K. E. France, P. B. McIntyre, E. Thébault & M. Loreau, 2007. The functional role of biodiversity in ecosystems: incorporating trophic complexity. Ecology Letters 10: 522–538. https://doi.org/10.1111/j.1461-0248.2007.01037.x.

Elrifi, I. R. & D. H. Turpin, 1985. Steady-state luxury consumption and the concept of optimum nutrient ratios: A study with phosphate and nitrate limited *Selenastrum minutum* (chlorophyta) 1. Journal of Phycology 21: 592–602. https://doi.org/10.1111/j.0022-3646.1985.00592.x.

Elser, J. J., D. R. Dobberfuhl, N. A. MacKay & J. H. Schampel, 1996. Organism size, life history, and N: P stoichiometry: toward a unified view of cellular and ecosystem processes. BioScience 46: 674–684. https://doi.org/10.2307/1312897.

Elser, J., R. Sterner, E. A. Gorokhova, W. Fagan, T. Markow, J. Cotner, J. Harrison, S. Hobbie, G. Odell & L. Weider, 2008. Biological stoichiometry from genes to ecosystems. Ecology Letters 3: 540–550. https://doi.org/10.1111/j.1461-0248.2000.00185.x.

Engel, A., 2000. The role of transparent exopolymer particles (TEP) in the increase in apparent particle stickiness (α) during the decline of a diatom bloom. Journal of Plankton Research 22: 485–497. https://doi.org/10.1093/plankt/22.3.485.

Flynn, K. J., J. A. Raven, T. A. V. Rees, Z. Finkel, A. Quigg & J. Beardall, 2010. Is the growth rate hypothesis applicable to microalgae? Journal of Phycology 46: 1–12. https://doi.org/10.1093/plankt/22.3.485.

Fowler, S. W. & G. A. Knauer, 1986. Role of large particles in the transport of elements and organic compounds through the oceanic water column. Progress in Oceanography 16: 147–194. https://doi.org/10.1016/0079-6611(86)90032-7.

Garcia, N. S., J. A. Bonachela & A. C. Martiny, 2016. Interactions between growth-dependent changes in cell size, nutrient supply and cellular elemental stoichiometry of marine Synechococcus. The ISME Journal 10: 2715–2724. https://doi.org/10.1038/ismej.2016.50.

Geider, R. & J. La Roche, 2002. Redfield revisited: variability of C: N: P in marine microalgae and its biochemical basis. European Journal of Phycology 37: 1–17. https://doi.org/10.1017/S0967026201003456.

Goldman, J. C., J. J. McCarthy & D. G. Peavey, 1979. Growth rate influence on the chemical composition of phytoplankton in oceanic waters. Nature 279: 210–215. https://doi.org/10.1038/279210a0.

Grasshoff, K., K. Kremling & M. Ehrhardt, 1999. Methods of seawater analysis, Wiley, VCH, Weinheim:

Groß, E., M. Boersma & C. L. Meunier, 2021. Environmental impacts on single-cell variation within a ubiquitous diatom: The role of growth rate. PloS ONE 16: e0251213. https://doi.org/10.1371/journal.pone.0251213.

Guillard, R. R., 1975. Culture of phytoplankton for feeding marine invertebrates Culture of marine invertebrate animals. Springer, 29–60. https://doi.org/10.1007/978-1-4615-8714-9_3.

Guillard, R. R. & J. H. Ryther, 1962. Studies of marine planktonic diatoms: I. Cyclotella nana Hustedt, and Detonula confervacea (Cleve) Gran. Canadian Journal of Microbiology 8: 229–239. https://doi.org/10.1139/m62-029.

Hantzsche, F. M. & M. Boersma, 2010. Dietary-induced responses in the phagotrophic flagellate Oxyrrhis marina. Marine Biology 157: 1641–1651. https://doi.org/10.1007/s00227-010-1437-1.

He, L., X. Han & Z. Yu, 2014. A rare *Phaeodactylum tricornutum* cruciform morphotype: culture conditions, transformation and unique fatty acid characteristics. PloS ONE 9: e93922. https://doi.org/10.1371/journal.pone.0093922.

Hillebrand, H. & B. Matthiessen, 2009. Biodiversity in a complex world: consolidation and progress in functional biodiversity research. Ecology Letters 12: 1405–1419. https://doi.org/10.1111/j.1461-0248.2009.01388.x.

Hillebrand, H., G. Steinert, M. Boersma, A. Malzahn, C. L. Meunier, C. Plum & R. Ptacnik, 2013. Goldman revisited: Faster-growing phytoplankton has lower N: P and lower stoichiometric flexibility. Limnology and Oceanography 58: 2076–2088. https://doi.org/10.4319/lo.2013.58.6.2076.

Isanta-Navarro, J., C. Prater, L. M. Peoples, I. Loladze, T. Phan, P. D. Jeyasingh, M. J. Church, Y. Kuang & J. J. Elser, 2022. Revisiting the growth rate hypothesis: Towards a holistic stoichiometric understanding of growth. Ecology Letters 25: 2324–2339. https://doi.org/10.1111/ele.14096.

Klausmeier, C. A., E. Litchman & S. A. Levin, 2004. Phytoplankton growth and stoichiometry under multiple nutrient limitation. Limnology and Oceanography 49: 1463–1470. https://doi.org/10.4319/lo.2004.49.4_part_2.1463.

Klein, C., P. Claquin, A. Pannard, C. Napoléon, B. Le Roy & B. Véron, 2011. Dynamics of soluble extracellular polymeric substances and transparent exopolymer particle pools in coastal ecosystems. Marine Ecology Progress Series 427: 13–27. https://doi.org/10.3354/meps09049.

Kremp, A., A. Godhe, J. Egardt, S. Dupont, S. Suikkanen, S. Casabianca & A. Penna, 2012. Intraspecific variability in the response of bloom-forming marine microalgae to changed climate conditions. Ecology and Evolution 2: 1195–1207. https://doi.org/10.1002/ece3.245.

Litchman, E. & C. A. Klausmeier, 2008. Trait-based community ecology of phytoplankton. Annual Review of Ecology, Evolution, and Systematics 39: 615–639. https://doi.org/10.1146/annurev.ecolsys.39.110707.173549.

Litchman, E., C. A. Klausmeier, O. M. Schofield & P. G. Falkowski, 2007. The role of functional traits and trade-offs in structuring phytoplankton communities: scaling from cellular to ecosystem level. Ecology Letters 10: 1170–1181. https://doi.org/10.1111/j.1461-0248.2007.01117.x.

Loladze, I. & J. J. Elser, 2011. The origins of the Redfield nitrogen-to-phosphorus ratio are in a homoeostatic protein-to-rRNA ratio. Ecology Letters 14: 244–250. https://doi.org/10.1111/j.1461-0248.2010.01577.x.

Lønborg, C., M. Middelboe & C. P. Brussaard, 2013. Viral lysis of Micromonas pusilla: impacts on dissolved organic matter production and composition. Biogeochemistry 116: 231–240. https://doi.org/10.1007/s10533-013-9853-1.

Maat, D. S. & C. P. Brussaard, 2016. Both phosphorus-and nitrogen limitation constrain viral proliferation in marine phytoplankton. Aquatic Microbial Ecology 77: 87–97. https://doi.org/10.3354/ame01791.

Maat, D. S., K. J. Crawford, K. R. Timmermans & C. P. Brussaard, 2014. Elevated CO_2 and phosphate limitation favor Micromonas pusilla through stimulated growth and reduced viral impact. Applied and Environmental Microbiology 80: 3119–3127. https://doi.org/10.1128/AEM.03639-13.

Malzahn, A. M., N. Aberle, C. Clemmesen & M. Boersma, 2007. Nutrient limitation of primary producers affects planktivorous fish condition. Limnology and Oceanography 52: 2062–2071. https://doi.org/10.4319/lo.2007.52.5.2062.

Malzahn, A. M. & M. Boersma, 2012. Effects of poor food quality on copepod growth are dose dependent and non-reversible. Oikos 121: 1408–1416. https://doi.org/10.1111/j.1600-0706.2011.20186.x.

Marie, D., N. Simon & D. Vaulot, 2005. Phytoplankton cell counting by flow cytometry. Algal Culturing Techniques 1: 253–267.

Martino, A. D., A. Meichenin, J. Shi, K. Pan & C. Bowler, 2007. Genetic and phenotypic characterization of *Phaeodactylum tricornutum* (Bacillariophyceae) accessions 1. Journal of Phycology 43: 992–1009. https://doi.org/10.1111/j.1529-8817.2007.00384.x.

Martiny, A. C., G. I. Hagstrom, T. DeVries, R. T. Letscher, G. L. Britten, C. A. Garcia, E. Galbraith, D. Karl, S. A. Levin & M. W. Lomas, 2022. Marine phytoplankton resilience may moderate oligotrophic ecosystem responses and biogeochemical feedbacks to climate change. Limnology and Oceanography 67: S378–S389. https://doi.org/10.1002/lno.12029.

Massie, T. M., B. Blasius, G. Weithoff, U. Gaedke & G. F. Fussmann, 2010. Cycles, phase synchronization, and entrainment in single-species phytoplankton populations. Proceedings of the National Academy of Sciences 107: 4236–4241. https://doi.org/10.1073/pnas.0908725107.

McBeain, K. A. & K. H. Halsey, 2018. Altering phytoplankton growth rates changes their value as food for microzooplankton grazers. Aquatic Microbial Ecology 82: 19–29. https://doi.org/10.3354/ame01880.

McGregor, G. B. & B. C. Sendall, 2021. True branching and phenotypic plasticity in the planktonic cyanobacterium Dolichospermum brachiatum sp. nov. (Nostocales, Aphanizomenonaceae), from south-eastern Australia. Phytotaxa 491: 93–114. https://doi.org/10.11646/phytotaxa.491.2.1.

Meunier, C. L., F. M. Hantzsche, A. Ö. Cunha-Dupont, J. Haafke, B. Oppermann, A. M. Malzahn & M. Boersma, 2012. Intraspecific selectivity, compensatory feeding and flexible homeostasis in the phagotrophic flagellate Oxyrrhis marina: three ways to handle food quality fluctuations. Hydrobiologia 680: 53–62. https://doi.org/10.1007/s10750-011-0900-4.

Moore, J. K., W. Fu, F. Primeau, G. L. Britten, K. Lindsay, M. Long, S. C. Doney, N. Mahowald, F. Hoffman & J. T. Randerson, 2018. Sustained climate warming drives declining marine biological productivity. Science 359: 1139–1143. https://doi.org/10.1126/science.aao6379.

Moorthi, S. D., J. A. Schmitt, A. Ryabov, I. Tsakalakis, B. Blasius, L. Prelle, M. Tiedemann & D. Hodapp, 2016. Unifying ecological stoichiometry and metabolic theory to predict production and trophic transfer in a marine planktonic food web. Philosophical Transactions of the Royal Society b: Biological Sciences 371: 20150270. https://doi.org/10.1098/rstb.2015.0270.

Peñuelas, J., B. Poulter, J. Sardans, P. Ciais, M. Van Der Velde, L. Bopp, O. Boucher, Y. Goddéris, P. Hinsinger & J. Llusia, 2013. Human-induced nitrogen–phosphorus imbalances alter natural and managed ecosystems across the globe. Nature Communications 4: 1–10. https://doi.org/10.1038/ncomms3934.

Peñuelas, J., J. Sardans, A. Rivas-ubach & I. A. Janssens, 2012. The human-induced imbalance between C, N and P in Earth's life system. Global Change Biology 18: 3–6. https://doi.org/10.1111/j.1365-2486.2011.02568.x.

Plum, C. & H. Hillebrand, 2019. Multiple zooplankton species alter the stoichiometric interactions between producer and consumer levels. Marine Biology 166: 163. https://doi.org/10.1007/s00227-019-3609-y.

Ptacnik, R., A. G. Solimini, T. Andersen, T. Tamminen, P. Brettum, L. Lepistö, E. Willén & S. Rekolainen, 2008. Diversity predicts stability and resource use efficiency in natural phytoplankton communities. Proceedings of the National Academy of Sciences 105: 5134–5138. https://doi.org/10.1073/pnas.0708328105.

Redfield, A. C., 1958. The biological control of chemical factors in the environment. American Scientist 46: 230A-A221.

Reusch, T. B. & P. W. Boyd, 2013. Experimental evolution meets marine phytoplankton. Evolution 67: 1849–1859. https://doi.org/10.1111/evo.12035.

Rhee, G. Y., 1978. Effects of N: P atomic ratios and nitrate limitation on algal growth, cell composition, and nitrate uptake. Limnology and Oceanography 23: 10–25. https://doi.org/10.4319/lo.1978.23.1.0010.

Rhee, G. Y. & I. J. Gotham, 1980. Optimum N: P ratios and coexistence of planktonic algae. Journal of Phycology 16: 486–489. https://doi.org/10.1111/j.1529-8817.1980.tb03065.x.

Rogers, C. E., C. Navas, K. F. Bush & J. Dyble Bressie, 2012. A novel, transportable flow cytometer facilitates algal quantification in cultures and environmental samples.

Technical Bulletin, BD Biosciences: https://www.bdbio
sciences.com/content/dam/bdb/marketing-documents/
Accuri-TB-Algal-Quantifi-in-Cultures-and-Env-Samples.
pdf.

Song, Z., G. J. Lye & B. M. Parker, 2020. Morphological and biochemical changes in *Phaeodactylum tricornutum* triggered by culture media: Implications for industrial exploitation. Algal Research 47: 101822. https://doi.org/10.1016/j.algal.2020.101822.

Sterner, R. W. & J. J. Elser, 2002. Ecological stoichiometry: the biology of elements from molecules to the biosphere, Princeton University Press, Princeton, New Jersey, USA: https://doi.org/10.1515/9781400885695.

Striebel, M., S. Schabhüttl, D. Hodapp, P. Hingsamer & H. Hillebrand, 2016. Phytoplankton responses to temperature increases are constrained by abiotic conditions and community composition. Oecologia 182: 815–827. https://doi.org/10.1007/s00442-016-3693-3.

Thébault, E. & M. Loreau, 2005. Trophic interactions and the relationship between species diversity and ecosystem stability. The American Naturalist 166: E95–E114. https://doi.org/10.1086/444403.

Thébault, E. & M. Loreau, 2006. The relationship between biodiversity and ecosystem functioning in food webs. Ecological Research 21: 17–25. https://doi.org/10.1007/s11284-005-0127-9.

Thingstad, T. F., L. Øvreås, J. K. Egge, T. Løvdal & M. Heldal, 2005. Use of non-limiting substrates to increase size; a generic strategy to simultaneously optimize uptake and minimize predation in pelagic osmotrophs? Ecology Letters 8: 675–682. https://doi.org/10.1111/j.1461-0248.2005.00768.x.

Thrane, J. E., D. O. Hessen & T. Andersen, 2016. The impact of irradiance on optimal and cellular nitrogen to phosphorus ratios in phytoplankton. Ecology Letters 19: 880–888. https://doi.org/10.1111/ele.12623.

Utermöhl, H., 1958. Zur vervollkommnung der quantitativen phytoplankton-methodik: Mit 1 Tabelle und 15 abbildungen im Text und auf 1 Tafel. Internationale Vereinigung Für Theoretische Und Angewandte Limnologie: Mitteilungen 9: 1–38.

Vallina, S. M., P. Cermeno, S. Dutkiewicz, M. Loreau & J. M. Montoya, 2017. Phytoplankton functional diversity increases ecosystem productivity and stability. Ecological Modelling 361: 184–196. https://doi.org/10.1016/j.ecolmodel.2017.06.020.

Volcani, B., 1981. Cell wall formation in diatoms: morphogenesis and biochemistry Silicon and siliceous structures in biological systems. Springer, 157–200.

Weaver, W. & C. Shannon, (1963). The mathematical theory of communication University of Illinois Press Urbana.

West-Eberhard, M. J., 2003. Developmental plasticity and evolution, Oxford University Press:

Xue, J., Y.-F. Niu, T. Huang, W.-D. Yang, J.-S. Liu & H.-Y. Li, 2015. Genetic improvement of the microalga *Phaeodactylum tricornutum* for boosting neutral lipid accumulation. Metabolic Engineering 27: 1–9. https://doi.org/10.1016/j.ymben.2014.10.002.